



OPEN ACCESS

EDITED BY

Frank Van Bel,
University Medical Center Utrecht, Netherlands

REVIEWED BY

MaryAnn Volpe,
Tufts University, United States
Chung-Ming Chen,
Taipei Medical University, Taiwan

*CORRESPONDENCE

Dongmei Yue
yuedm@sj-hospital.org

SPECIALTY SECTION

This article was submitted to Neonatology,
a section of the journal Frontiers in Pediatrics

RECEIVED 09 April 2022

ACCEPTED 21 September 2022

PUBLISHED 10 October 2022

CITATION

Zuo J, Tong Y, Yang Y, Wang Y and Yue D (2022)
Claudin-18 expression under hyperoxia in
neonatal lungs of bronchopulmonary dysplasia
model rats.
Front. Pediatr. 10:916716.
doi: 10.3389/fped.2022.916716

COPYRIGHT

© 2022 Zuo, Tong, Yang, Wang and Yue. This is
an open-access article distributed under the
terms of the [Creative Commons Attribution
License \(CC BY\)](https://creativecommons.org/licenses/by/4.0/). The use, distribution or
reproduction in other forums is permitted,
provided the original author(s) and the
copyright owner(s) are credited and that the
original publication in this journal is cited, in
accordance with accepted academic practice.
No use, distribution or reproduction is
permitted which does not comply with these
terms.

Claudin-18 expression under hyperoxia in neonatal lungs of bronchopulmonary dysplasia model rats

Jingye Zuo, Yajie Tong, Yuting Yang, Yirui Wang
and Dongmei Yue*

Department of Pediatrics, Shengjing Hospital of China Medical University, Shenyang, China

Background: Bronchopulmonary dysplasia (BPD) is characterized by impaired alveolar and microvascular development. Claudin-18 is the only known lung-specific tight junction protein affecting the development and transdifferentiation of alveolar epithelium.

Objective: We aimed to explore the changes in the expression of claudin-18, podoplanin, SFTPC, and the canonical WNT pathway, in a rat model of hyperoxia-induced BPD, and to verify the regulatory relationship between claudin-18 and the canonical WNT pathway by cell experiments.

Methods: A neonatal rat and cell model of BPD was established by exposing to hyperoxia (85%). Hematoxylin and eosin (HE) staining was used to confirm the establishment of the BPD model. The mRNA levels were assessed using quantitative real-time polymerase chain reaction (qRT-PCR). Protein expression levels were determined using western blotting, immunohistochemical staining, and immunofluorescence.

Results: As confirmed by HE staining, the neonatal rat model of BPD was successfully established. Compared to that in the control group, claudin-18 and claudin-4 expression decreased in the hyperoxia group. Expression of β -catenin in the WNT signaling pathway decreased, whereas that of p-GSK- 3β increased. Expression of the AEC II marker SFTPC initially decreased and then increased, whereas that of the AEC I marker podoplanin increased on day 14 ($P < 0.05$). Similarly, claudin-18, claudin-4, SFTPC and β -catenin were decreased but podoplanin was increased when AEC line RLE-6TN exposed to 85% hyperoxia. And the expression of SFTPC was increased, the podoplanin was decreased, and the WNT pathway was upregulated when claudin-18 was overexpressed.

Conclusions: Claudin-18 downregulation during hyperoxia might affect lung development and maturation, thereby resulting in hyperoxia-induced BPD. Additionally, claudin-18 is associated with the canonical WNT pathway and AECs transdifferentiation.

KEYWORDS

bronchopulmonary dysplasia, claudin-18, canonical WNT pathway, AEC transdifferentiation, claudin-4

Introduction

Bronchopulmonary dysplasia (BPD) is one of the most common chronic respiratory diseases in preterm infants. Lung injury caused by inflammation is the key factor in BPD (1, 2), the typical pathological feature of which is the interruption of alveolar and capillary development. Pulmonary edema is the main manifestation of BPD in the early stage (3). Alveolar epithelial barrier is a sealed interface between adjacent epithelial cells, whose damage could lead to pulmonary edema, and its function depends on tight junctions—a type of transmembrane protein complex.

The claudin family of membrane proteins plays a central role in the structure and function of tight junctions (4). In humans, claudin-1, 3–5, 7, 8, 10, 12, 18, and 23 are most abundantly expressed (5). Studies in rats demonstrate that alveolar epithelial cells (AECs) I and II primarily express claudin-3, 4, and 18 (6). However, only claudin-18.1, one of the isomers of claudin-18, is known to be specifically expressed in lung tissues (7), indicating its lung-specific functions.

The canonical WNT pathway has been reported to be extensively involved in lung cell proliferation, migration, invasion, and apoptosis (8–10), playing a key role in the patterning of early lung organogenesis (11). WNT signaling in epithelial and mesenchymal cells peaks at the onset of the tubular phase, declines sharply in the mid-tubular phase, and remains low during the cystic and alveolar phases (12). Wnt3a can regulate the proliferation and differentiation of AECII to AECI in hyperoxia-induced BPD (13).

Many studies have proven that the claudin family is closely related to the WNT/ β -catenin pathway. Regulation of claudin-18 is involved in the JAM axis and closely related to the WNT/ β -catenin pathway (14). JAM-A is a putative inhibitor of glycogen synthase kinase-3 β (GSK-3 β) (15). And mice with low expression of JAM-A have been reported to show increased sensitivity to lung injury (16). Therefore, JAM-A might have a protective effect against acute lung injury by stimulating alveolar epithelial tight junctions. The purinergic receptor P2X7, representing an ATP-gated ionotropic receptor, affects the WNT/ β -catenin signaling pathway in AECs under conditions of injury (17). Expression of claudin-18 in the lungs of P2X7 $^{-/-}$ mice has been reported to be increased, and the expression of GSK-3 β protein and its inactive form in AECs also increased, suggesting that claudin-18 is negatively correlated with P2X7 receptor expression and positively correlated with GSK-3 β expression related (18). Precisely coordinated activation of the WNT/ β -catenin signaling pathway is critical for normal lung development. Aberrantly activated β -catenin patterns have been reported in human BPD tissues and in hyperoxia models of BPD. Increased plasma wnt5a in hyperoxia-induced lung cystic hyperplasia could promote alveolarization and septal

thickening in BPD patients (19). However, the mechanism by which the WNT pathway specifically regulates claudin-18 expression still remains unclear.

AECs are injured when exposed to hyperoxia, which might lead to the pathogenesis of BPD, which is regulated by many factors, such as connective tissue growth factor (20), Nrf2 (21), and silencing information regulator 2 related enzyme 1 (22) and so on. Claudin-18 is an important component of pulmonary tight junction proteins involved in permeability regulation and barrier function, and it has also been shown to be involved in the process of alveolar development (23). Claudin-4 is a type of transmembrane protein that promotes fluid-clearance function to maintain function of lung epithelial barrier (24, 25). We hypothesized that claudin-18 downregulation during hyperoxia could affect lung development and contribute to hyperoxia-induced BPD. And claudin-18 is associated with the canonical WNT pathway and AECs transdifferentiation (Figure 1). In this study, we assessed the changes in claudin-18, claudin-4, SFTPC, podoplanin, GSK-3 β , p-GSK-3 β , and β -catenin expression levels in the lungs of neonatal rat model of hyperoxia-induced BPD compared to that in control rats. Additionally, we aimed to study the development of alveoli, to further illustrate the role of claudin-18 in the pathophysiological process of hyperoxia-induced BPD.

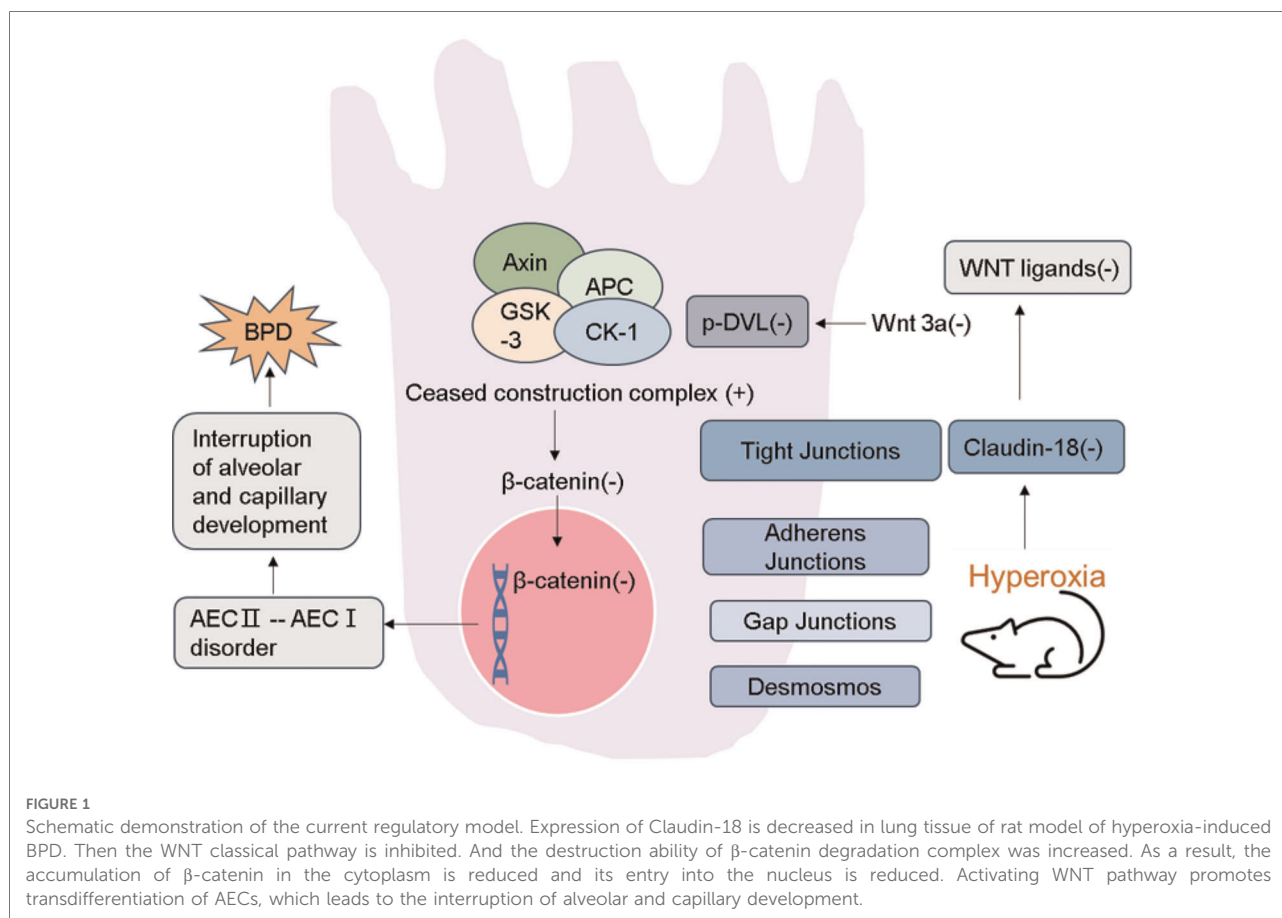
Materials and methods

Experimental subjects and groups

All animal experiments were performed in accordance with the National Institutes of Health guidelines and protocols approved by the Institutional Animal Care and Use Committee (approval no. 2020PS574K). Forty Sprague–Dawley rats (10-week-old; Changsheng Co., Ltd. Shenyang, China) were mated at a male to female ratio of 1:4. Female rats were separated after conception. Within 12 h of the pregnant female rats naturally giving birth, neonatal rats were randomly divided into two groups namely Con (21% O₂, $n = 50$) and BPD (80%–85% O₂, $n = 50$). The newborn rats, along with their mother rats were exposed to normoxia or hyperoxia until postnatal day 14. The lactating mother rats were switched between normoxia and hyperoxia every 24 h to avoid oxygen poisoning. All animals had a 12-h light/dark cycle, with free drinking water and standard diet (23).

Tissue harvest

Ten neonatal rats were randomly selected on postnatal days 1, 3, 7, 10, and 14 (Supplementary Figure S1) for harvesting



their lungs. The thoracic cavity was opened after euthanasia by isoflurane (2%) inhalation, and the right ventricle was perfused. When lungs became white, they were collected aseptically. For preparing paraffin specimens for hematoxylin and eosin (HE) staining, immunohistochemistry (IHC), and immunofluorescence (IF), the right lower lobe was fixed in 4% paraformaldehyde without dissection, dehydrated using graded alcohol, and rendered transparent using xylene. The remaining lobes were quick-frozen in liquid nitrogen and stored at -80°C for subsequent western blot analysis and qPCR.

Determination of wet and dry weights

To determine the wet and dry weights, the upper right lobe was collected and weighed as wet weight. It was then placed in an oven at 80°C for 24 h, and then weighed again. This step was repeated until the weight of the lung lobe changed no further, and dry weight was obtained. The psychrometric ratio, given by $(\text{wet weight} - \text{dry weight}) / \text{dry weight}$, was calculated to assess the degree of pulmonary edema.

Hematoxylin and eosin (He) staining and radical alveolar count (RAC)

Paraffin blocks of lung tissues were sliced into $2.5\text{-}\mu\text{m}$ thick sections for HE staining. Radical alveolar count (RAC; Wang et al. 2019) was determined as follows: Based on the HE-stained specimens, a straight line was drawn directly between the centre of the respiratory bronchioles and the nearest fibrous septum, and the number of alveoli through which the line passed were counted. RAC was determined using a light microscope (magnification, $100\times$) by counting each slice thrice and averaging the obtained values.

Quantitative real-time PCR

Total RNA was extracted from lung tissues using the RNAiso Plus (Code No9108, TaKaRa Bio, Japan), and concentration and purity of the isolated RNA were measured using a NanoDrop spectrophotometer (Thermo Fisher Scientific, MA, USA). For removing genomic DNA contamination and reverse-

transcribing the obtained RNA, the PrimeScript™ RT reagent kit with gDNA Eraser kit (Code No. RR047A, Takara Bio, Japan) was used. PCR amplification was conducted using qPCR premix (Code No. RR820A, Takara Bio, Japan). Primers were designed by Sangon Biotech; the sequences and other details are shown as follows: Rat ACTB Endogenous Reference Genes Primers (Order NO. B661202, Sangon Biotech); claudin-18 PCR primers: GCTCTGTTTGTGGGCT GGATCG (forward) and GAAGTTGCGGTCATCAG GA GTCAG (reverse); claudin-4 PCR primers: TCATCGGCAGCAACATCGTCAC (forward) and GCC AGCATCG AGTCGTACATCTTG (reverse); SFTPC PCR primers: CCCAGGAGCCAGTTTCGC ATTC(forward) and GACGACAAGGACTACCACCACAAC (reverse); podoplanin PCR primers: C CTCCGACCACGAT CACAAAGAAC (forward) and CACCGCCT GCGTTAT CTCTATTGG (reverse); β -catenin PCR primers: TACCGCT GGGACCC TACACAAC(forward) and GCG TGGTGATGGC GTAGAACAG (reverse).

The cycle threshold (Ct) value was considered acceptable for analysis. ACTB was used as the reference gene, and the $2^{-\Delta\Delta Ct}$ method was used to evaluate the relative changes in levels of each gene. All data shown represent the average results from three replicates.

Western blot analysis

Total protein was extracted from the lung tissue, and its concentration was determined using an enhanced BCA kit (Beyotime Biotechnology). Thereafter, 30 μ g of the protein sample was subjected to 10% SDS-polyacrylamide gel electrophoresis, followed by transfer of the separated proteins to a polyvinylidene fluoride membrane (ISEQ00010, Millipore, USA) (26). After blocking with 5% skim milk at 37 °C for 2 h, the membrane was incubated with anti-claudin-18 (1:1,000, Abcam, USA), anti-claudin-4 (1:1,000, Invitrogen, USA), anti-SFTPC (1:1,000, Proteintech, China), anti-podoplanin (1:1,000, Santa Cruz, USA), anti-GSK-3 β (1:1,000, CST, USA), anti-p-GSK-3 β (1:1,000, CST, USA), and anti- β -catenin (1: 1,000, CST, USA) antibodies overnight at 4 °C. The next day, membranes were incubated with the corresponding horseradish peroxidase-conjugated secondary antibody (S0001, S0002, Affinity) at 37 °C for 2 h. Amersham Imager 600 (GE Healthcare Life Sciences) was used to detect chemiluminescence signals, and the Image J 1.8.0 was used to calculate the gray value. The experiment was repeated at least thrice.

Immunohistochemical staining

Paraffin sections were deparaffinized, incubated with Tris-EDTA antigen retrieval solution, and blocked with anti-claudin-18 (1:200), anti-claudin-4 (1:100), anti-SFTPC

(1:100), anti-podoplanin (1:200), and anti- β -catenin (1:100) antibodies at 4 °C overnight. Images were acquired and analysed using Image Pro Plus 6.0 to assess protein expression.

Immunofluorescence staining

Paraffin sections (2.5- μ m thick) were deparaffinized, washed with PBS, heat-repaired, and blocked with 3% Triton-X in 10% goat serum at room temperature for 1 h. The specimens were then incubated with anti-claudin-18 (1:200), anti- β -catenin (1:100), or anti-podoplanin-antibodies (1:100) overnight at 4 °C. The next day, sections were incubated with Alexa Fluor 488- and Alexa Fluor 594-conjugated secondary antibodies (1:400, Abcam) for 4 h at 37 °C. Sections were subjected to DAPI staining for 5 min, following which they were mounted with glycerol and visualized under a full spectrum laser confocal microscope (C1Si, Nikon, Japan).

Cell culture and transfection

The RLE-6TN cell line was purchased from Bena Culture Collection and cultured in RPMI 1,640 medium (Gibco) with 10% fetal bovine serum (Clark). The control group was maintained in a humidified incubator with 21% O₂ while the BPD group was kept at 37 °C with 85% O₂, and cells were collected after 24 h. The cells were transfected with negative control (NC) plasmid to form the P-NC group, and with claudin18 overexpression plasmid synthesized by Hanheng Co., Ltd. to generate the claudin18 group. Transfections were performed using Lipo 3,000 (Invitrogen) according to the manufacturer's instruction.

Statistical analysis

The data obtained in the experiment were all analysed using Prism 8.0. A t-test was performed while assessing two groups, whereas one-way analysis of variance (ANOVA) was performed for comparing multiple groups, and repeated measures ANOVA was employed for comparing two groups at different time points. Statistical significance was set at 0.05.

Results

Pulmonary edema and alveolar dysfunction observed in the neonatal rat model of hyperoxia-induced BPD

The survival rate of neonatal rats was 100% in both control group and BPD group. Lung tissues of neonatal rats in the

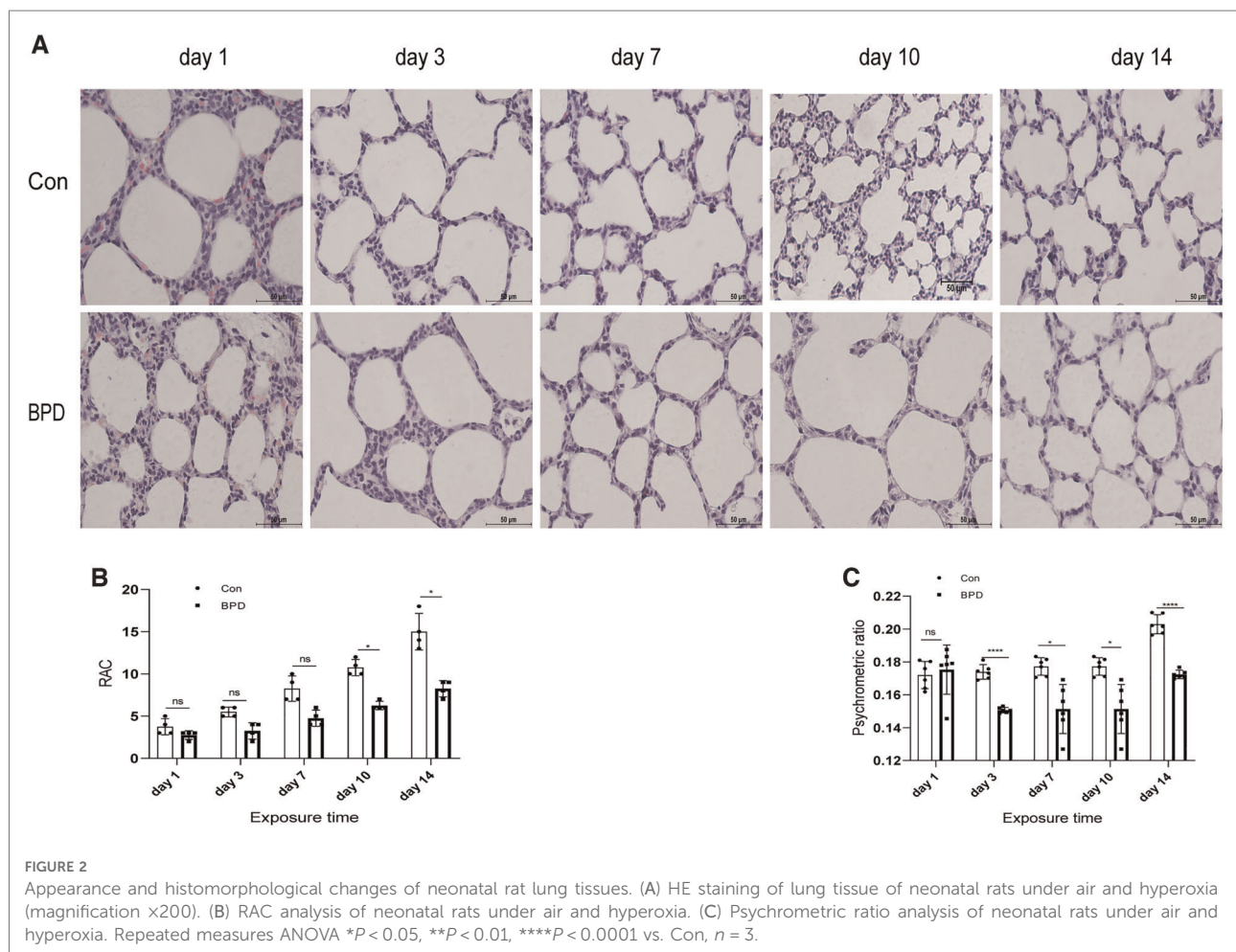
hyperoxia group showed evident edema and immature alveolar development. Histopathological results showed that, with increase in age, alveolar cavity of the air group rats increased in number and decreased in size; the alveolar compartments increased in number and gradually became thinner. In the BPD group, alveolar development gradually became disordered, volume of the alveolar cavity became larger with evident alveolar fusion, interstitial cell proliferation, and simultaneous inflammatory cell infiltration (Figures 2A,B). Psychrometric ratio analysis suggested that the degree of lung tissue edema in neonatal rats of the BPD group was significantly higher than that in the control group (Figure 2C).

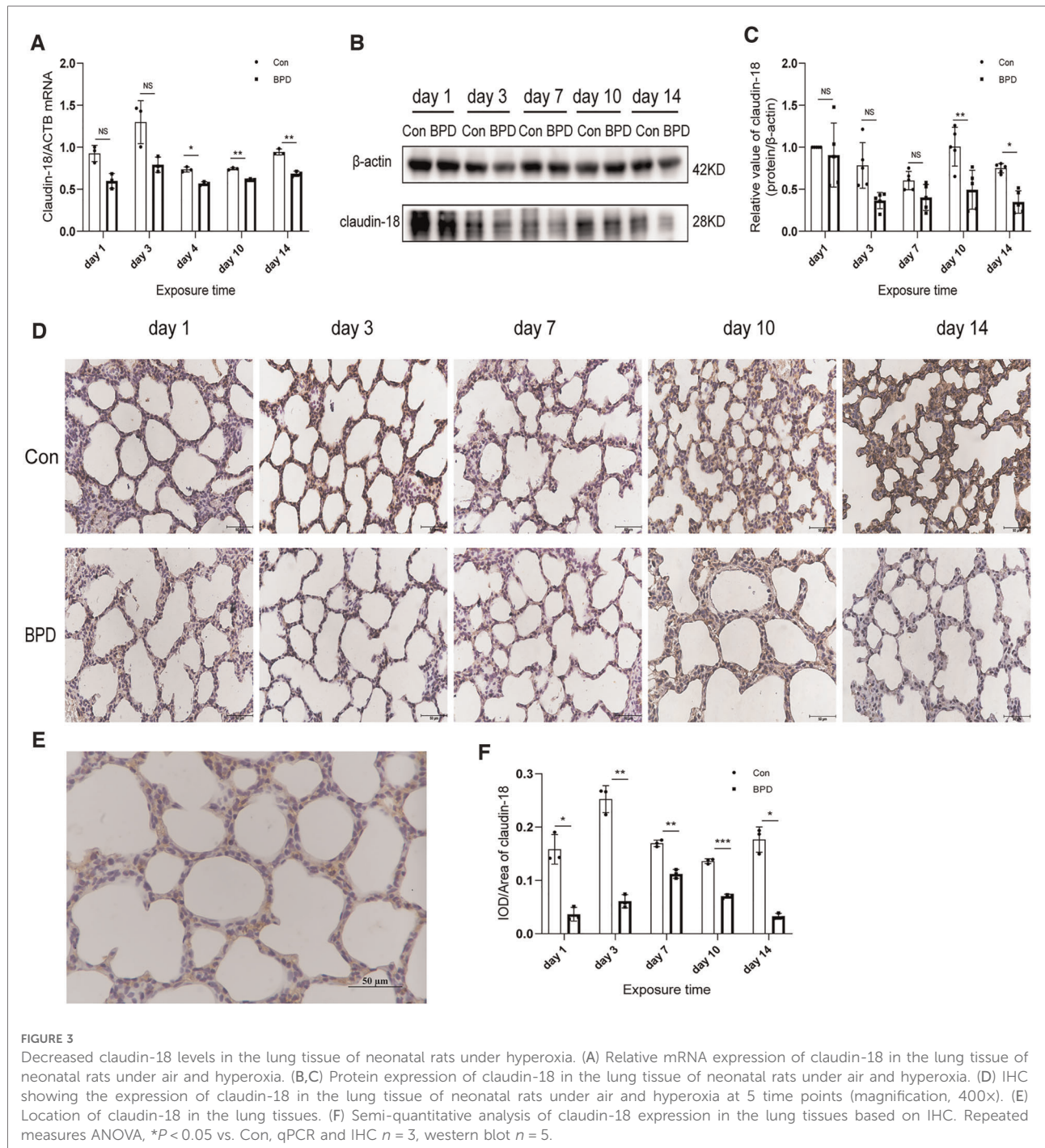
Down-regulation of claudin-18 and claudin-4 in the rat model of hyperoxia-induced BPD

To determine the role of claudin-18 in BPD model induced by hyperoxia, we used different methods to detect the expression of claudin-18 (Figure 3) and claudin-4 (Figure 4) in neonatal lung tissues. QPCR results showed that claudin-18

transcription in the neonatal lung of the control group to be significantly higher than that in the BPD group ($P < 0.05$) (Figure 3A). Western blot experiments showed that, compared to the air group, claudin-18 expression was significantly reduced, to varying degrees, under hyperoxia ($P < 0.05$) (Figures 3B,C). IHC results showed claudin-18 to mainly be expressed in the cytoplasm of AECs (Figures 3D,E). Semi-quantitative analysis showed claudin-18 expression in lung tissues of the air group to be significantly higher than that in the BPD group ($P < 0.05$) (Figure 3F). The experimental results are perfectly uniform, seemingly proving that hyperoxia affects claudin-18 expression in pulmonary tissues.

We next used the three methods mentioned above to detect claudin-4, another important member of the claudin family. QPCR results showed that claudin-4 transcription in the air group was significantly higher than that in the hyperoxia group on days 10 and 14; however, no difference in claudin-4 expression was noted between the air and hyperoxia groups on postnatal days 1, 3, and 7 ($P > 0.05$) (Figure 4A). Western blot results showed no significant difference in claudin-4 expression between these two groups on postnatal days 1 and 7 ($P > 0.05$). However, claudin-4 expression in the control

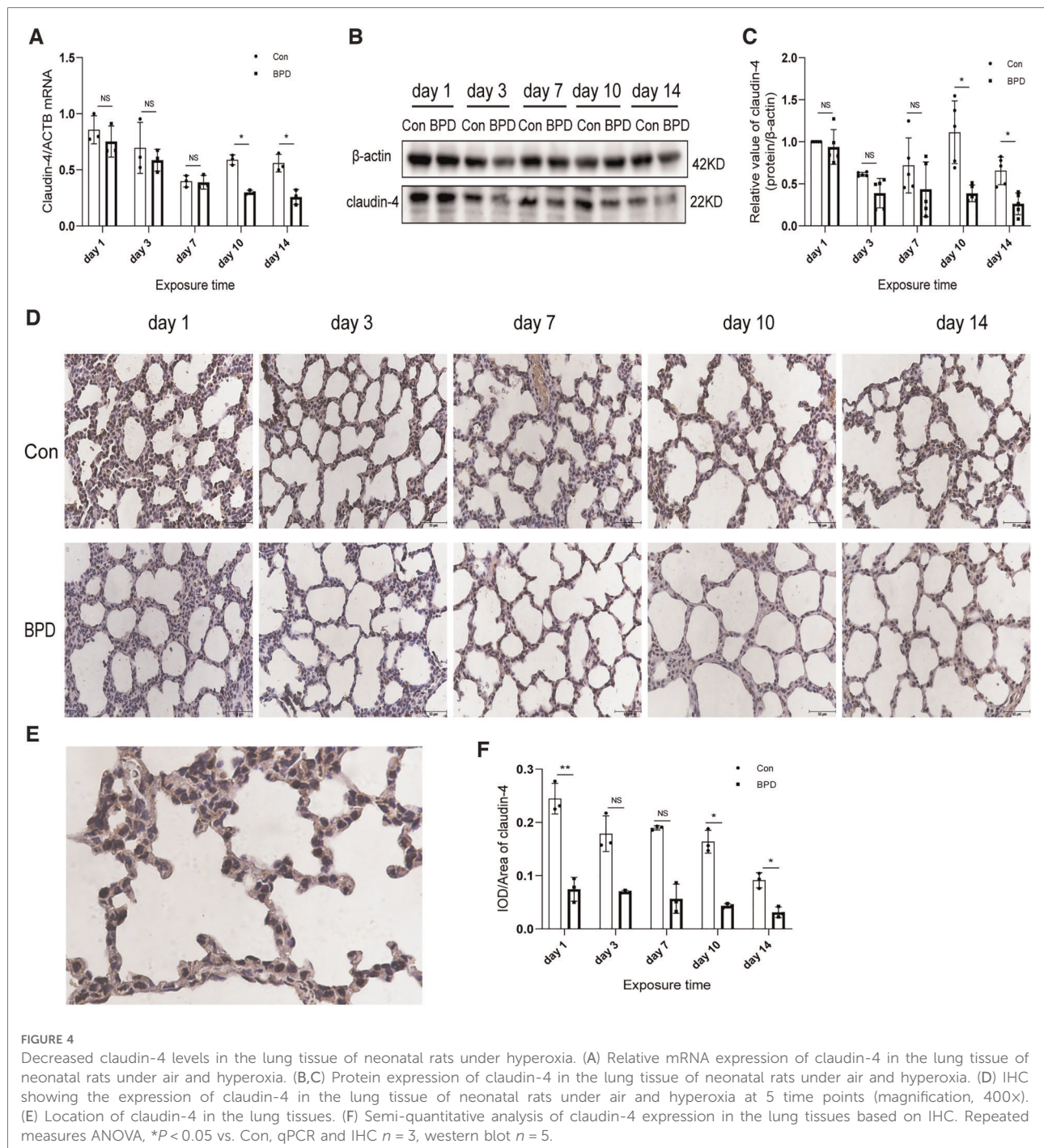




group was significantly higher than that in BPD group on postnatal days 10 and 14 ($P < 0.05$) (Figures 4B,C). IHC showed claudin-4 to be primarily expressed in the cytoplasm of AECs (Figures 4D,E); claudin-4 expression in the hyperoxia group was significantly lower than that in the air group ($P < 0.05$) (Figure 4F). Expression of claudin-18 and claudin-4 was decreased in the rat model of hyperoxia-induced BPD.

Podoplanin and SFTPC expression in the rat model of hyperoxia-induced BPD

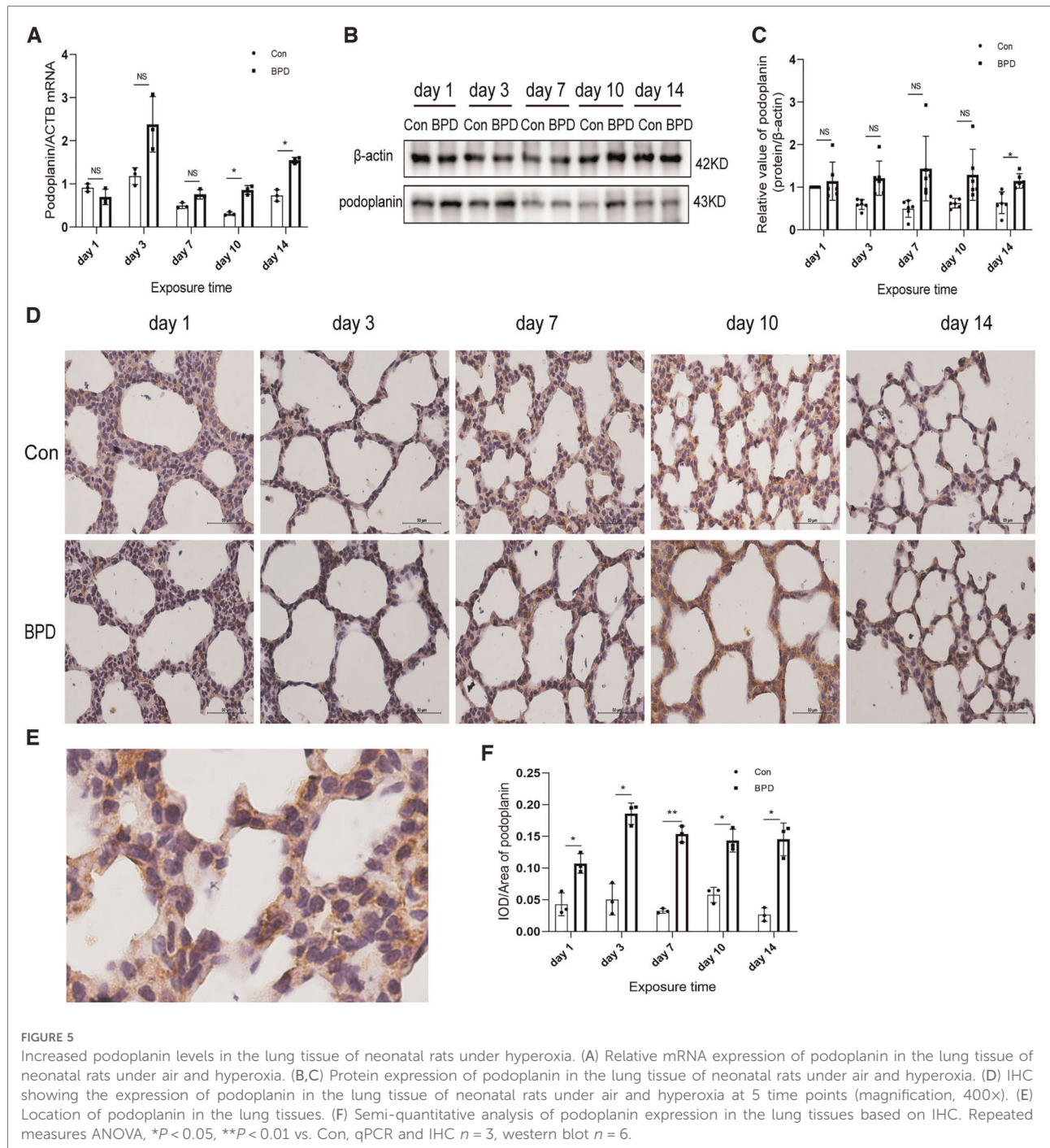
We tested the expression of marker proteins AEC I-podoplanin and AEC II-SFTPC to confirm the transdifferentiation of AECs under hyperoxia (Figures 5, 6). QPCR results showed that podoplanin in the hyperoxia group to be significantly higher than that in the air group on days 10 and



14 (Figure 5A). Western blot results showed podoplanin expression to only be increased significantly on postnatal day 14, with no difference in the expression levels between the hyperoxia and air groups on days 1, 3, 7, and 10 (Figures 5B,C). Similar to the qPCR results, IHC showed that under hyperoxia, podoplanin expression was significantly increased (Figures 5D–F).

The SFTPC transcription in neonatal lungs of the hyperoxia group was significantly lower than that in the air group on postnatal days 3, 7, and 10 while being

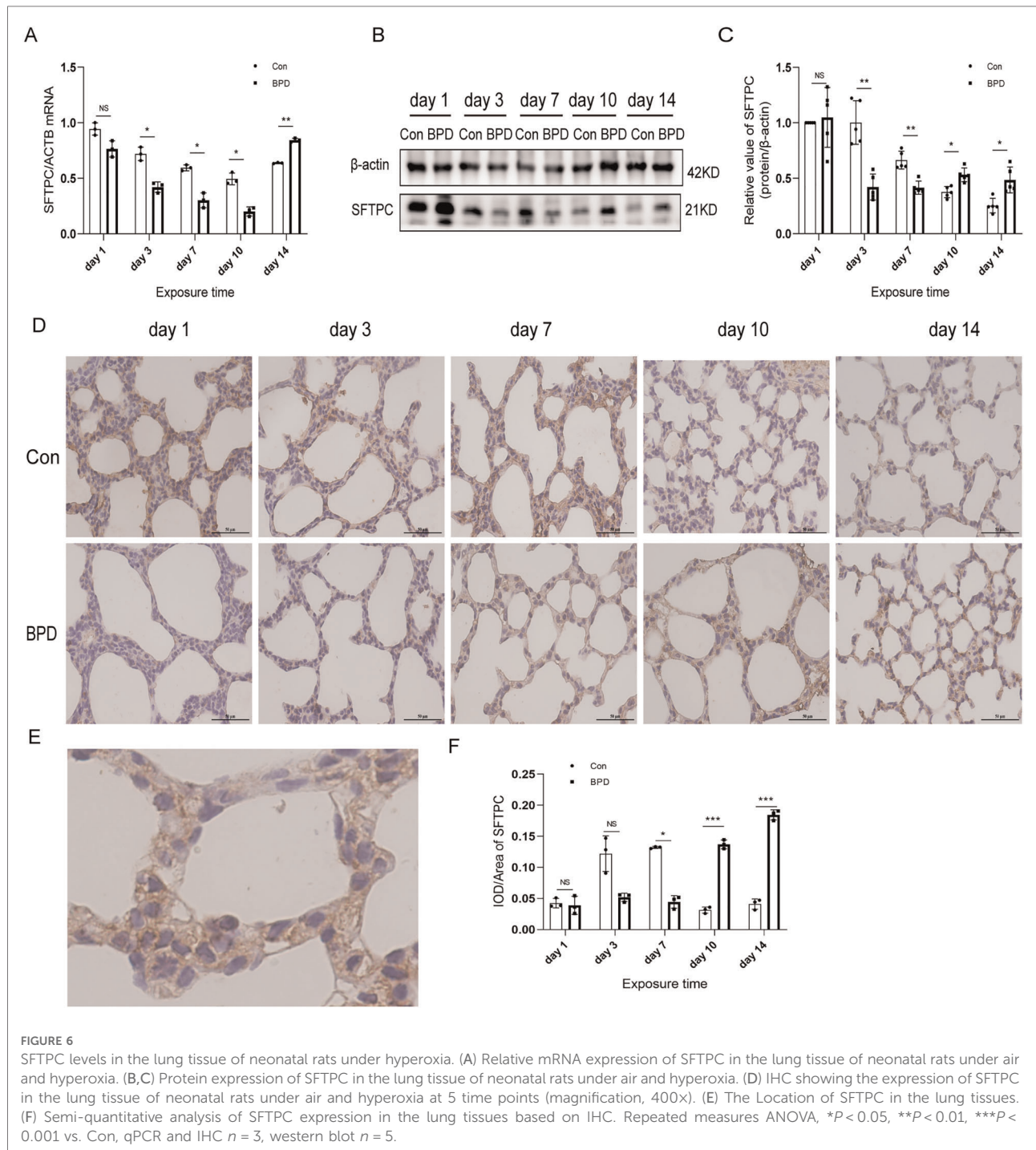
significantly higher on day 14 (Figure 6A). Western blot results suggested that SFTPC expression in the BPD group was significantly lower than that in the control group on postnatal days 3 and 7, whereas it was significantly higher in the BPD group on postnatal days 10 and 14 (Figures 6B,C). IHC suggested that SFTPC was expressed in both nucleus and cytoplasm (Figures 6D,E). The semi-quantitative analysis results were consistent with the western blot results (Figure 6F).



Inhibition of the canonical WNT pathway in the rat model of hyperoxia-induced BPD

We found that the WNT pathway was downregulated under hyperoxia (Figure 7). Moreover, the mRNA expression of β -catenin in the hyperoxia group was found to be significantly lower than that in the air group (Figure 7A). Western blot

results showed no significant difference in β -catenin expression between the two groups on postnatal day 3; however, the expression in the hyperoxia group was significantly lower than that in the air group on postnatal days 1, 7, 10, and 14 and β -catenin level was dramatically reduced on day 14 (Figures 7B, C). Further, the relative protein expression of p-GSK-3 β significantly increased on days 10 and 14 (Figure 7D). IHC showed β -catenin to be expressed in both the nucleus and the



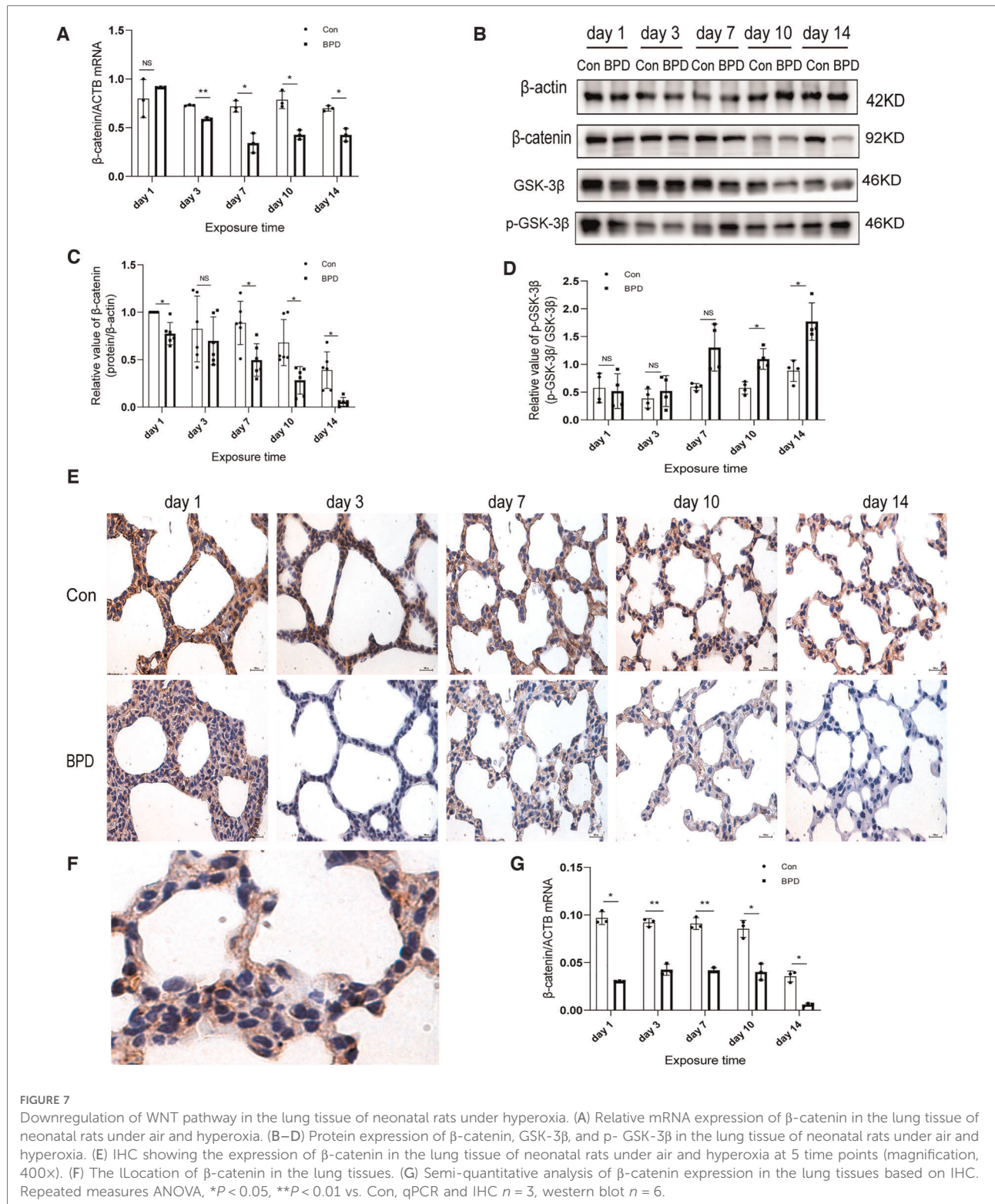
cytoplasm (Figures 7E,F). Under hyperoxia, β -catenin expression was significantly reduced (Figure 7G).

Correlation between claudin-18 and β -catenin expression in neonatal lungs

Double IF staining was performed to locate claudin-18 and podoplanin in pulmonary tissues (Figure 8A). Claudin-18 was

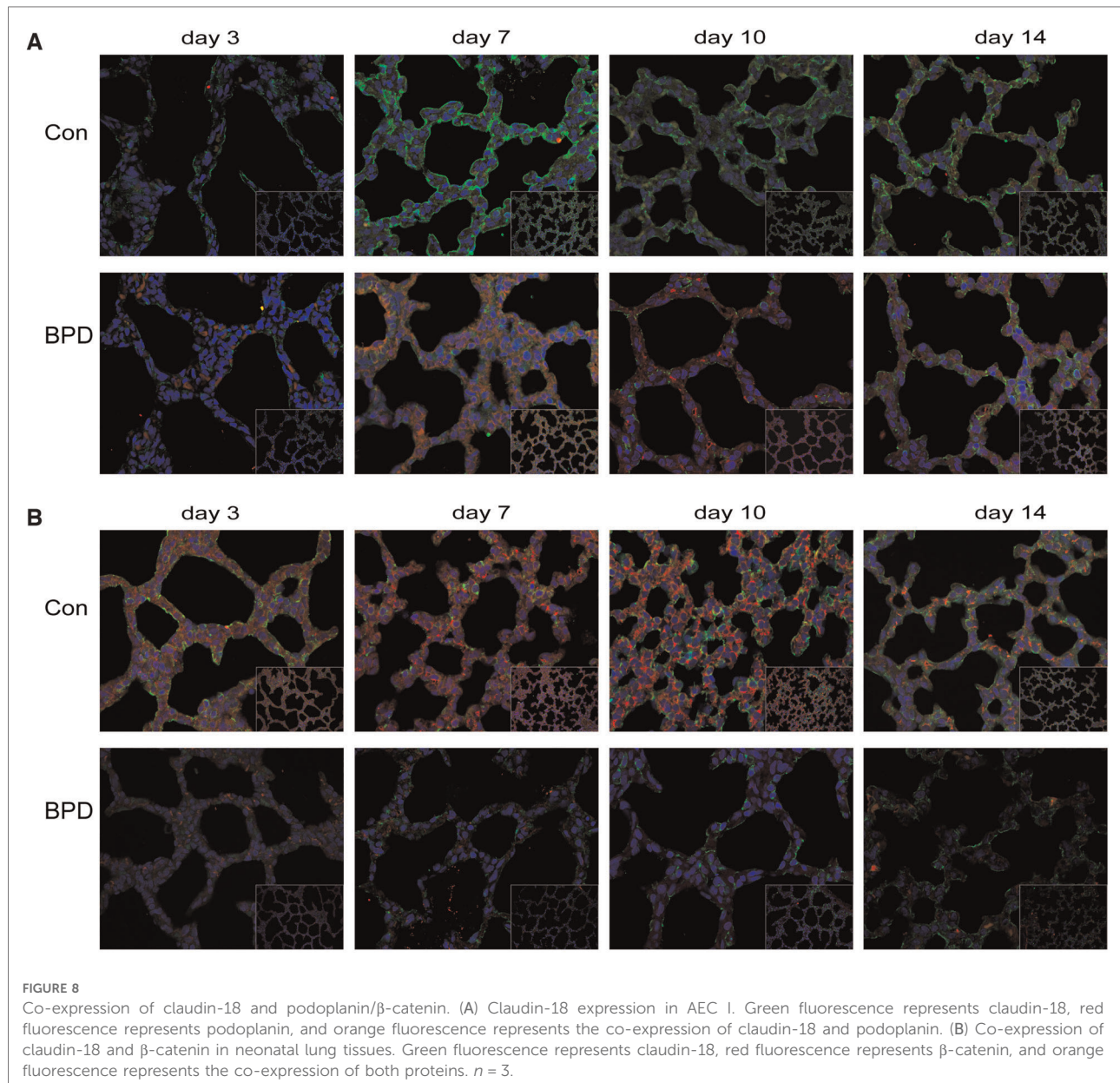
mainly expressed in the cytoplasm along the cell membrane, while podoplanin was mainly expressed within the cytoplasm. At the same time point, green fluorescence intensity of claudin-18 was higher in the Con group than that in the BPD group. As red fluorescence intensity of podoplanin was lower in the Con group, the overall colour was greener. Whereas fluorescence of the BPD group was reddish.

To observe the effect of hyperoxia on claudin-18 and β -catenin expression, we performed double IF staining of



claudin-18 and β -catenin (Figure 8B). As seen earlier, claudin-18 was mainly expressed along the edge of the cytoplasmic cell membrane, whereas β -catenin was diffusely expressed in the cytoplasm. Fluorescence intensity of both was greatly reduced

under hyperoxia. The red fluorescence representing by β -catenin underwent greater reduction, and fluorescence of the air group was, therefore, orange, whereas that of BPD group was green.



We conducted Pearson's correlation analysis on claudin-18 and β -catenin expression based on the western blot results and found a significant positive correlation between the two ($r = 0.286$, $P < 0.05$) (**Supplementary Figure S2**).

Influence of claudin-18 overexpression on the WNT pathway and AECs transdifferentiation

To verify the results of animal experiments, we established a BPD cell model. Our experimental results showed the expression of claudin-18, SFTPC and β -catenin to decrease and the that of podoplanin to increase under hyperoxia, which was consistent with the results of animal experiments (**Figures 9A–E**).

Next, we constructed a claudin18 overexpression plasmid to explore the effect of claudin18 on the canonical WNT pathway and AECs transdifferentiation (**Figures 9F–J**). Overexpression of claudin-18 increased the expression of SFTPC and decreased that of podoplanin, suggesting the transdifferentiation of AECs to have weakened. At the same time, the expression of β -catenin was increased, which suggested the WNT pathway to be activated.

Discussion

In this study, we aimed to determine the role of claudin-18 in the pathophysiology of hyperoxia-induced BPD using a suitable neonatal rat model. Claudin-18 was found to be

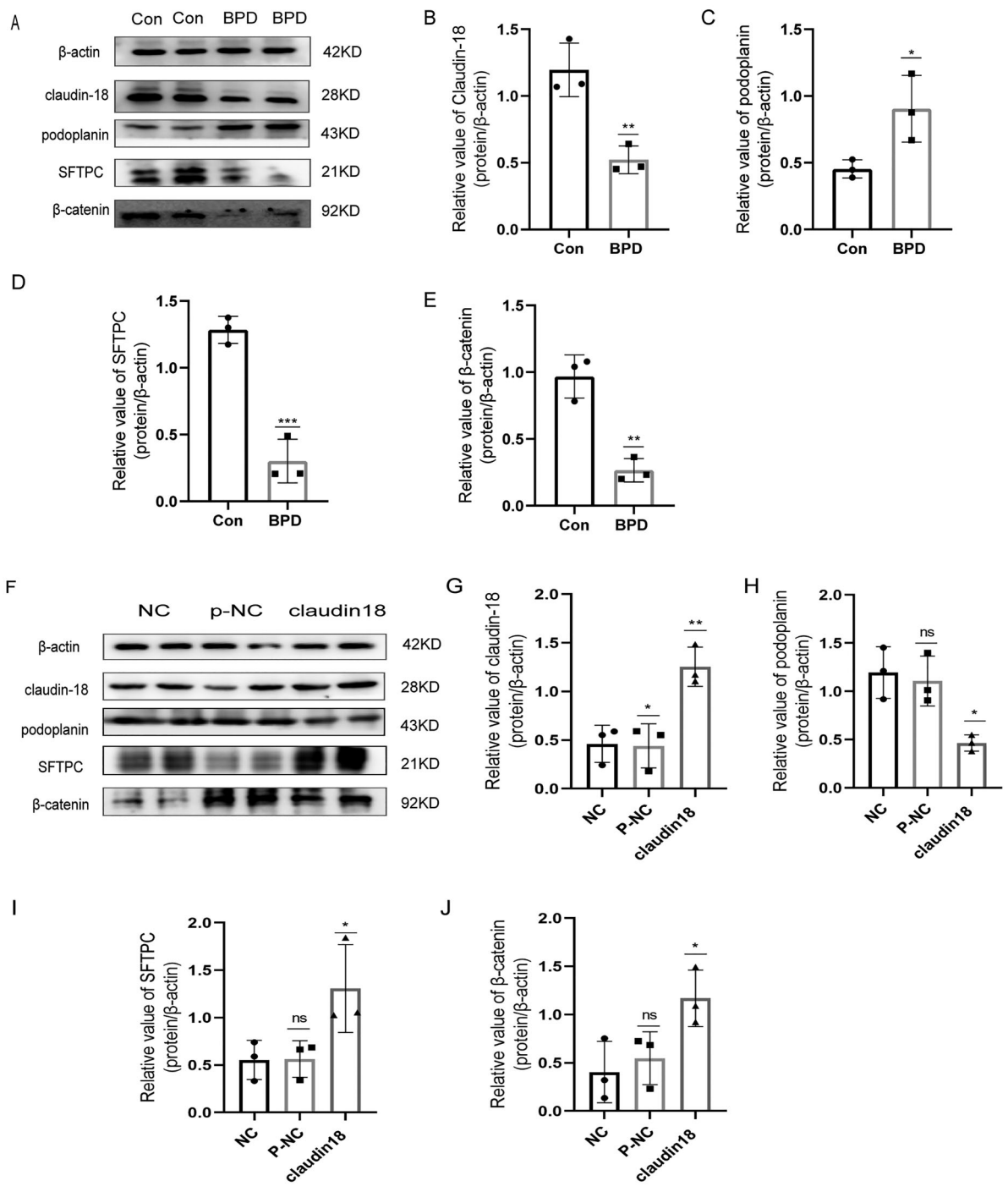


FIGURE 9 Effects of hyperoxia and claudin-18 overexpression on WNT pathway and AECs transdifferentiation. (A–E) Protein levels of podoplanin, SFTPC, and β-catenin upon hyperoxia. T-test analysis, * $P < 0.05$, ** $P < 0.01$, *** $P < 0.001$ vs. Con, $n = 3$. (F–J) Protein levels of podoplanin, SFTPC, and β-catenin after overexpression plasmid transfection. One-way ANOVA, * $P < 0.05$, ** $P < 0.01$ vs. Con, $n = 3$.

mainly distributed along the edge of the cell membrane in the cytoplasm. Compared to that in the control group, claudin-18 expression showed a significant decrease under hyperoxia. SFTPC expression was reduced on postnatal days 3 and 7 and

increased on postnatal days 10 and 14. Podoplanin expression was increased on postnatal day 14. Our preliminary study revealed that transdifferentiation of AECs is abnormally strengthened under hyperoxia. And we found that classic

WNT/ β -catenin pathway is inhibited under hyperoxia. To investigate the effect of claudin-18 on WNT pathway and AECs transdifferentiation, we transfected claudin-18 overexpression plasmid and found that WNT pathway was activated and AECs transdifferentiation decreased compared with the control group. Therefore, claudin-18 may affect the transdifferentiation of AECs through the WNT pathway, resulting in alveolar dysplasia.

The spatiotemporal expression pattern of claudin-18 during lung development is highly regulated. From embryonic day 16.5 to postnatal day 15, its expression shows an upward trend. Except for postnatal day 3, claudin-18 expression first declines and then reaches a peak at postnatal on day 1 (27). In various animal models of lung injury, decreased expression of claudin-18 has been considered a sign of lung barrier damage (28–31). Especially in a model of hyperoxia-induced BPD, claudin-18 has been shown to possibly be involved in early pulmonary edema development and late alveolar development (32).

Michael et al. (23) studied the role of claudin-18 in lung development and barrier function by producing a claudin-18 (exon 2 and 3) knock-out (KO) mouse model. They found that, compared to wild-type mice, claudin-18 KO mice had lung injury and pulmonary edema, severity of which increased with time, along with an increased alveolar epithelial barrier permeability. When AECs were formed in claudin-18 KO mice, an increase in radial perinuclear aggregates associated with the nuclear plasma membrane was reportedly observed (33). Changes in morphology and function of tight junctions noted in the claudin-18 KO mouse model, namely fewer alveoli, larger in size, widened alveolar compartments, and impaired alveolar formation, were similar to those observed in the rat model of hyperoxia-induced BPD. Human fetal alveoli at a gestational age of 23–24 weeks, which are in the small vesicle stage and still immature, show a state of atelectasis, with widened alveolar interval and increased alveolar fluid exudation. The changes occurred within the risk period of BPD development (34) and may be related to abnormal claudin expression.

Our study showed increased SFTPC expression in neonatal lungs under hyperoxia. Although the transdifferentiation from AEC II to AEC I was thought to be enhanced under these conditions, the expression of SFTPC was decreased in the early stage, which increased later, contrasting the expected trend of transdifferentiation enhancement. The results are consistent with those obtained in previous studies. Hou et al. (35) found SFTPC expression in tissues to first decrease and then increase, while that of the AEC I marker, AQP5, increased in the BPD model. However, primary cells isolated from lung tissues indicated the decreasing trend of SFTPC expression and increasing trend of AQP5 expression. The underlying reason could be that when AEC II

transdifferentiation to AEC I increases in tissues, AEC II proliferation is required to maintain the number of cells.

Claudin-18 expression was deemed to be related to peripheral lung epithelial cell maturation (36). Drugs that promote lung maturation could induce claudin-18 expression in human fetal AECs and promote alveolar development, suggesting that claudin-18 may be a potential driver of lung maturation (37). Furthermore, compared to the wild-type group, higher expression of pro-SPC and podoplanin was observed in the claudin-18 KO mouse model (23). Researchers speculated that KO of claudin-18 could have resulted in abnormal AEC differentiation. However, the extent to which claudin-18 expression affects AEC phenotype would need further investigation, and the mechanisms underlying barrier dysfunction and AEC damage remain to be clarified.

In our study, the WNT signalling pathway was inhibited under hyperoxia, possibly enhancing AEC II transdifferentiation. Inhibition of this pathway could reduce cell proliferation, promoting AEC II differentiation to AEC I (38). The expression of β -catenin in embryonic lung respiratory epithelial cells is necessary for the growth and differentiation of peripheral epithelial cell progenitor cells (39, 40). The absence of β -catenin in embryonic lung epithelial cells disrupts lung morphogenesis, restricts the formation and differentiation of peripheral lungs, and enhances the formation of conductive airways (41).

Many recent studies have reported that the WNT signalling pathway is activated by hyperoxia (42–44). Our results differed from the previous ones in at least two aspects. First, we tested five time points after birth, representing a critical period of lung development, when the normal development of the lung is ensured by precise regulation of the WNT pathway. In addition, experiments yielding opposite results were conducted under the intervention of different drugs. Further, despite the BPD model being established in a manner similar to that in previous studies, the feeding conditions and animal batches used were different.

This was the first study that used a neonatal rat model of hyperoxia-induced BPD to investigate the effect of claudin-18 on rat AECs transdifferentiation. And we confirmed that overexpressing claudin-18 could activate WNT and inhibit AECs transdifferentiation. However, a limitation of the study was that we are not sure whether claudin-18 inhibits AECs transdifferentiation by activating canonical WNT pathway, which needs more efforts to explore the molecular mechanisms underlying the obtained results.

Conclusions

In a neonatal rat model of hyperoxia-induced BPD, changes in claudin-18 and claudin-4 expression were found to follow the

same trend as that in the WNT signaling pathway, co-occurring with abnormal AEC transdifferentiation. Therefore, claudin family may be a potential regulator of the WNT canonical pathway, and possibly playing a unique role in AEC transdifferentiation. Nonetheless, this hypothesis warrants further experimental validation.

Data availability statement

The original contributions presented in the study are included in the article/**Supplementary Material**, further inquiries can be directed to the corresponding author/s.

Ethics statement

The animal study was reviewed and approved by National Institutes of Health guidelines and protocols approved by the Institutional Animal Care and Use Committee (approval no. 2020PS574K).

Author contributions

JZ and DY conceived the experiments, JZ conducted the experiments, YT analysed the raw data, YY provided reagents and materials, YW was responsible for the original draft preparation. All authors have reviewed the results and agreed to the published version of the manuscript. All authors contributed to the article and approved the submitted version.

References

1. Kalikkot Thekkevedu R, Guaman MC, Shivanna B. Bronchopulmonary dysplasia: a review of pathogenesis and pathophysiology. *Respir Med.* (2017) 132:170–7. doi: 10.1016/j.rmed.2017.10.014
2. Papagianis PC, Pillow JJ, Moss TJ. Bronchopulmonary dysplasia: pathophysiology and potential anti-inflammatory therapies. *Paediatr Respir Rev.* (2019) 30:34–41. doi: 10.1016/j.prrv.2018.07.007
3. Bhandari A, Bhandari V. Pathogenesis, pathology and pathophysiology of pulmonary sequelae of bronchopulmonary dysplasia in premature infants. *Front Biosci.* (2003) 8:e370–80. doi: 10.2741/1060
4. Xu YN, Deng MS, Liu YF, Yao J, Xiao ZY. Tight junction protein CLDN17 serves as a tumor suppressor to reduce the invasion and migration of oral cancer cells by inhibiting epithelial-mesenchymal transition. *Arch Oral Biol.* (2021) 133:105301. doi: 10.1016/j.archoralbio.2021.105301
5. Schlingmann B, Molina SA, Koval M. Claudins: gatekeepers of lung epithelial function. *Semin Cell Dev Biol.* (2015) 42:47–57. doi: 10.1016/j.semcdb.2015.04.009
6. LaFemina MJ, Rokkam D, Chandrasena A, Pan J, Bajaj A, Johnson M, et al. Keratinocyte growth factor enhances barrier function without altering claudin expression in primary alveolar epithelial cells. *Am J Physiol Lung Cell Mol Physiol.* (2010) 299(6):L724–34. doi: 10.1152/ajplung.00233.2010
7. Türeci O, Koslowski M, Helftenbein G, Castle J, Rohde C, Dhaene K, et al. Claudin-18 gene structure, regulation, and expression is evolutionary conserved in mammals. *Gene.* (2011) 481(2):83–92. doi: 10.1016/j.gene.2011.04.007
8. Aros CJ, Pantoja CJ, Gomperts BN. WNT signaling in lung development, regeneration, and disease progression. *Commun Biol.* (2021) 4(1):601. doi: 10.1038/s42003-021-02118-w
9. Li Z, Fang F, Xu F. Effects of different states of oxidative stress on fetal rat alveolar type II epithelial cells in vitro and ROS-induced changes in WNT signaling pathway expression. *Mol Med Rep.* (2013) 7(5):1528–32. doi: 10.3892/mmr.2013.1388
10. Raslan AA, Yoon JK. WNT signaling in lung repair and regeneration. *Mol Cells.* (2020) 43(9):774–83. doi: 10.14348/molcells.2020.0059
11. Goss AM, Morrisey EE. WNT signaling and specification of the respiratory endoderm. *Cell Cycle.* (2010) 9(1):10–1. doi: 10.4161/cc.9.1.10272
12. Ring DB, Johnson KW, Henriksen EJ, Nuss JM, Goff D, Kinnick TR, et al. Selective glycogen synthase kinase 3 inhibitors potentiate insulin activation of glucose transport and utilization in vitro and in vivo. *Diabetes.* (2003) 52(3):588–95. doi: 10.2337/diabetes.52.3.588
13. Jia X, Wu B, Huang J, Fan L, Yang M, Xu W. YAP and Wnt3a independently promote AECIIs proliferation and differentiation by increasing nuclear β -catenin expression in experimental bronchopulmonary dysplasia. *Int J Mol Med.* (2021) 47(1):195–206. doi: 10.3892/ijmm.2020.4791
14. Barth K, Bläsche R, Neißer A, Bramke S, Frank JA, Kasper M. P2X7R-dependent regulation of glycogen synthase kinase 3 β and claudin-18 in alveolar epithelial type I cells of mice lung. *Histochem Cell Biol.* (2016) 146(6):757–68. doi: 10.1007/s00418-016-1499-3

Funding

This research was supported by the Department of Science and Technology of Liaoning Province (grant number 2020 JH2/10300128) and Natural Science Foundation of Liaoning Province (grant number 201602873).

Conflict of interest

The authors declare that the research was conducted in the absence of any commercial or financial relationships that could be construed as a potential conflict of interest.

Publisher's note

All claims expressed in this article are solely those of the authors and do not necessarily represent those of their affiliated organizations, or those of the publisher, the editors and the reviewers. Any product that may be evaluated in this article, or claim that may be made by its manufacturer, is not guaranteed or endorsed by the publisher.

Supplementary material

The Supplementary Material for this article can be found online at: <https://www.frontiersin.org/articles/10.3389/fped.2022.916716/full#supplementary-material>.

15. Bazzoni G, Tonetti P, Manzi L, Cera MR, Balconi G, Dejana E. Expression of junctional adhesion molecule-A prevents spontaneous and random motility. *J Cell Sci.* (2005) 118(Pt 3):623–32. doi: 10.1242/jcs.01661
16. Mitchell LA, Ward C, Kwon M, Mitchell PO, Quintero DA, Nusrat A, et al. Junctional adhesion molecule A promotes epithelial tight junction assembly to augment lung barrier function. *Am J Pathol.* (2015) 185(2):372–86. doi: 10.1016/j.ajpath.2014.10.010
17. Barth K, Blasche R, Neisser A, Bramke S, Frank JA, Kasper M. Correction to: P2X7R-dependent regulation of glycogen synthase kinase 3beta and claudin-18 in alveolar epithelial type I cells of mice lung. *Histochem Cell Biol.* (2019) 151(3):277. doi: 10.1007/s00418-018-1758-6
18. Wesslau KP, Stein A, Kasper M, Barth K. P2X7 receptor indirectly regulates the JAM-A protein content via modulation of GSK-3beta. *Int J Mol Sci.* (2019) 20(9):2298. doi: 10.3390/ijms20092298
19. Sucre JMS, Jetter CS, Loomans H, Williams J, Plosa EJ, Benjamin JT, et al. Successful establishment of primary type II alveolar epithelium with 3D organotypic coculture. *Am J Respir Cell Mol Biol.* (2018) 59(2):158–66. doi: 10.1165/rcmb.2017-0442MA
20. Wang X, Cui H, Wu S. CTGF: a potential therapeutic target for bronchopulmonary dysplasia. *Eur J Pharmacol.* (2019) 860:172588. doi: 10.1016/j.ejphar.2019.172588
21. Ma D, Gao W, Liu J, Kong D, Zhang Y, Qian M. Mechanism of oxidative stress and Keap-1/Nrf2 signaling pathway in bronchopulmonary dysplasia. *Medicine.* (2020) 99(26):e20433. doi: 10.1097/MD.00000000000020433
22. Yang K, Dong W. SIRT1-related signaling pathways and their association with bronchopulmonary dysplasia. *Front Med.* (2021) 8:595634. doi: 10.3389/fmed.2021.595634
23. LaFemina MJ, Sutherland KM, Bentley T, Gonzales LW, Allen L, Chapin CJ, et al. Claudin-18 deficiency results in alveolar barrier dysfunction and impaired alveologenesis in mice. *Am J Respir Cell Mol Biol.* (2014) 51(4):550–8. doi: 10.1165/rcmb.2013-0456OC
24. Vyas-Read S, Vance RJ, Wang W, Colvocoresses-Dodds J, Brown LA, Koval M. Hyperoxia induces paracellular leak and alters claudin expression by neonatal alveolar epithelial cells. *Pediatr Pulmonol.* (2018) 53(1):17–27. doi: 10.1002/ppul.23681
25. Xu S, Xue X, You K, Fu J. Caveolin-1 regulates the expression of tight junction proteins during hyperoxia-induced pulmonary epithelial barrier breakdown. *Respir Res.* (2016) 17(1):50. doi: 10.1186/s12931-016-0364-1
26. Hu J, Wang J, Li C, Shang Y. Fructose-1,6-bisphosphatase aggravates oxidative stress-induced apoptosis in asthma by suppressing the Nrf2 pathway. *J Cell Mol Med.* (2021) 25(11):5001–14. doi: 10.1111/jcmm.16439
27. Lewis JB, Jimenez FR, Merrell BJ, Kimbler B, Arroyo JA, Reynolds PR. The expression profile of Claudin family members in the developing mouse lung and expression alterations resulting from exposure to secondhand smoke (SHS). *Exp Lung Res.* (2018) 44(1):13–24. doi: 10.1080/01902148.2017.1409846
28. Lee PH, Hong J, Jang AS. N-acetylcysteine decreases airway inflammation and responsiveness in asthma by modulating claudin 18 expression. *Korean J Intern Med.* (2020) 35(5):1229–37. doi: 10.3904/kjim.2019.105
29. T A MT, Ak G BS, Sks S. Curcumin prophylaxis refurbishes alveolar epithelial barrier integrity and alveolar fluid clearance under hypoxia. *Respir Physiol Neurobiol.* (2020) 274:103336. doi: 10.1016/j.resp.2019.103336
30. Reynolds CJ, Quigley K, Cheng X, Suresh A, Tahir S, Ahmed-Jushuf F, et al. Lung defense through IL-8 carries a cost of chronic lung remodeling and impaired function. *Am J Respir Cell Mol Biol.* (2018) 59(5):557–71. doi: 10.1165/rcmb.2018-0007OC
31. Weber B, Mendler MR, Lackner I, von Zelewski A, Hofler S, Baur M, et al. Lung injury after asphyxia and hemorrhagic shock in newborn piglets: analysis of structural and inflammatory changes. *PLoS One.* (2019) 14(7):e0219211. doi: 10.1371/journal.pone.0219211
32. Abdul-Hafez A, Mohamed T, Uhal BD. Activation of mas restores hyperoxia-induced loss of lung epithelial barrier function through inhibition of apoptosis. *J Lung Pulm Respir Res.* (2019) 6(3):58–62. doi: 10.15406/jlpr.2019.06.00208
33. Jin W, Rong L, Liu Y, Song Y, Li Y, Pan J. Increased claudin-3, -4 and -18 levels in bronchoalveolar lavage fluid reflect severity of acute lung injury. *Respirology.* (2013) 18(4):643–51. doi: 10.1111/resp.12034
34. Day CL, Ryan RM. Bronchopulmonary dysplasia: new becomes old again!. *Pediatr Res.* (2017) 81(1-2):210–3. doi: 10.1038/pr.2016.201
35. Hou A, Fu J, Yang H, Zhu Y, Pan Y, Xu S, et al. Hyperoxia stimulates the transdifferentiation of type II alveolar epithelial cells in newborn rats. *Am J Physiol Lung Cell Mol Physiol.* (2015) 308(9):L861–72. doi: 10.1152/ajplung.00099.2014
36. Shi F, Liao Y, Dong Y, Wang Y, Xie Y, Wan H. Claudin18 associated with corticosteroid-induced expression of surfactant proteins in pulmonary epithelial cells. *J Matern Fetal Neonatal Med.* (2019) 32(5):809–14. doi: 10.1080/14767058.2017.1392505
37. Niimi T, Nagashima K, Ward JM, Minoo P, Zimonjic DB, Popescu NC, et al. Claudin-18, a novel downstream target gene for the T/EBP/NKX2.1 homeodomain transcription factor, encodes lung- and stomach-specific isoforms through alternative splicing. *Mol Cell Biol.* (2001) 21(21):7380–90. doi: 10.1128/MCB.21.21.7380-7390.2001
38. Frank DB, Peng T, Zepp JA, Snitow M, Vincent TL, Penkala JJ, et al. Emergence of a wave of WNT signaling that regulates lung alveologenesis by controlling epithelial self-renewal and differentiation. *Cell Rep.* (2016) 17(9):2312–25. doi: 10.1016/j.celrep.2016.11.001
39. Ota C, Baarsma HA, Wagner DE, Hilgendorff A, Königshoff M. Linking bronchopulmonary dysplasia to adult chronic lung diseases: role of WNT signaling. *Mol Cell Pediatr.* (2016) 3(1):34. doi: 10.1186/s40348-016-0062-6
40. Mathew R. Signaling pathways involved in the development of bronchopulmonary dysplasia and pulmonary hypertension. *Children.* (2020) 7(8):100. doi: 10.3390/children7080100
41. Mucenski ML, Wert SE, Nation JM, Loudy DE, Huelsken J, Birchmeier W, et al. beta-catenin is required for specification of proximal/distal cell fate during lung morphogenesis. *J Biol Chem.* (2003) 278(41):40231–8. doi: 10.1074/jbc.M305892200
42. Alapati D, Rong M, Chen S, Hehre D, Rodriguez MM, Lipson KE, et al. Connective tissue growth factor antibody therapy attenuates hyperoxia-induced lung injury in neonatal rats. *Am J Respir Cell Mol Biol.* (2011) 45(6):1169–77. doi: 10.1165/rcmb.2011-0023OC
43. Alapati D, Rong M, Chen S, Lin C, Li Y, Wu S. Inhibition of LRP5/6-mediated WNT/ β -catenin signaling by Mesd attenuates hyperoxia-induced pulmonary hypertension in neonatal rats. *Pediatr Res.* (2013) 73(6):719–25. doi: 10.1038/pr.2013.42
44. Xu W, Zhao Y, Zhang B, Xu B, Yang Y, Wang Y, et al. Resveratrol attenuates hyperoxia-induced oxidative stress, inflammation and fibrosis and suppresses WNT/ β -catenin signalling in lungs of neonatal rats. *Clin Exp Pharmacol Physiol.* (2015) 42(10):1075–83. doi: 10.1111/1440-1681.12459